Experimental and numerical investigation of a novel non-catalytic reformer for methane partial oxidation

S. Benekos[1,*], A. Loukou[2,3], I. Frenzel[2], G. Skevis[4], M. Founti[1], D.Trimis[2,3],

[1]Mechanical Engineering Department, Laboratory of Heterogeneous Mixtures & Combustion Systems, Thermal Engineering Section, National Technical University of Athens, Greece
[2]Institute of Thermal Engineering, TU-Bergakademie Freiberg, Freiberg, Germany
[3]Engler-Bunte-Institute, Karlsruhe Institute of Technology, Karlsruhe, Germany
[4]Aerosol and Particle Technology Laboratory, Chemical Processes and Energy Resources Institute, Centre for Research and Technology Hellas, Thessaloniki, Greece

Abstract

The paper presents an experimental characterization and numerical simulation of a novel non-catalytic reformer design for methane partial oxidation with air that can potentially decrease the sooting propensity of the reforming process, while optimizing syngas efficiency. The first part of the paper provides details of the experimental procedure and presents temperature, pressure, species and soot measurements for a typical range of operation. A reformer efficiency of 65% was achieved at an air equivalence ratio of 0.5 and thermal load of 1.5kW under stationary operation in non-sooting conditions. The second part of the paper formulates an appropriate methodology for the numerical simulation of the reforming process based on a reactor network approach coupled with detailed gas-phase chemistry. Results indicate an accurate representation of the reforming process including acceptable agreement with experimental exhaust species levels.

Introduction

The development of clean, efficient and fuel flexible distributed energy production is crucial for successfully meeting the challenge of a sustainable energy future. Power systems based on solid oxide fuels cells (SOFC), fed by syngas (H_2/CO mixtures) have the potential of very high efficiencies at elevated operating temperatures (600-1000^{o}C). A limiting factor in SOFC system operation is the efficiency of the fuel reforming process. Optimized syngas production from methane reforming is an active area of research.

There are several reforming technologies such as steam, autothermal reforming and partial oxidation[1]. In particular, the exothermic partial oxidation process (POX) appears advantageous since there is no need for an external heat source or water balance. The process is essentially an under-stoichiometric combustion of the initial hydrocarbon fuel with oxygen or air and it can be conducted with or without the presence of a catalyst. The catalytic route known as CPOX, enhances the slow reforming reaction rates at lower temperatures, improves reforming efficiency and prevents soot formation. However, catalysts are sensitive against poisoning, get easily damaged by temperatures above 1000^{o}C and show a tendency to degenerate by age [2]. The non-catalytic route known as thermal partial oxidation (TPOX) is characterized by lower efficiency in comparison to the catalytic one but remains an interesting option due to fuel flexibility, potentially longer life times, good dynamic response and lower costs [3, 4]. However, the low adiabatic temperatures, slow chemical kinetics, flame instabilities and the persistent problem of soot formation are drawbacks which impede the development of TPOX reformers and they have to be addressed.

In earlier studies [5, 6] a practical solution to cope with the issue of soot formation was suggested, which was the use of a ceramic wall-flow filter (Figure 1), similar to the diesel particulate filters used in automotive applications, for soot retention from the syngas.

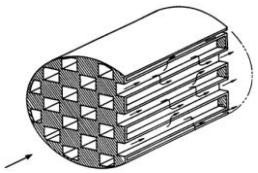

Figure 1: Schematic representation of the wall flow filter

However, the retention of soot particles in such filters causes increase in backpressure. The removal of accumulated soot within the filter is not a trivial issue. Conventional soot regeneration with oxygen or air is not possible in fuel cell based systems since it would lead to the oxidation of the Ni-based fuel cell anode catalyst. Another approach, that has already been proposed by the authors [5, 6], is a passive regeneration on the basis of gasification reactions (R.1, R.2) between the soot and gaseous species in the syngas that flows through the filter at high temperatures (> 800°C).

$$C + H_2O \Rightarrow CO + H_2 \quad (\Delta H=172 \text{ kJ/mol}) \quad (R.1)$$

$$C + CO_2 \Rightarrow 2CO \quad (\Delta H=131 \text{ kJ/mol}) \quad (R.2)$$

The present work attempts to combine this passive regeneration of the soot with the thermal partial oxidation process itself within a novel reformer design. In this reformer, the wall-flow filter is positioned within the reaction zone (Figure 2), where the temperature levels are high enough for soot regeneration.

The objective of the present work is to investigate the performance of the reformer experimentally and to set up a numerical model, which can be used for analyzing the process further and for optimizing eventually the design of the reformer.

Corresponding author: sot.benekos@gmail.com

Process characteristics such as temperature profiles, syngas composition and pressure drop within the filter were measured experimentally for operation with rich methane/air mixtures. The air ratio and thermal load were varied in order to study their influence on the dynamics of soot formation/ regeneration and on the efficiency of the reformer.

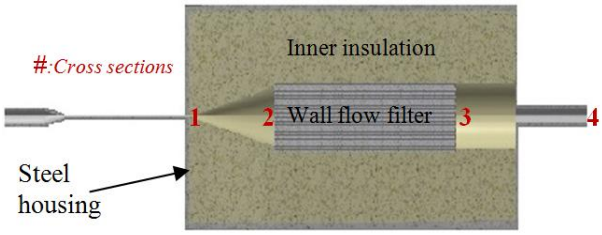

Figure 2: The non-catalytic reformer design.

For the particular design, the optimization of reforming efficiency and soot loading is influenced by thermodynamic, kinetic and flow (mainly residence time) parameters. A comprehensive optimization process would ideally involve a fully coupled 3D simulation of the reforming process. This is currently not feasible mainly due to limitations in computational power. Therefore, a different approach was chosen where the study of turbulent flow and detailed chemistry was decoupled. In such an approach the reformer is modeled as an equivalent Reactor Network (RN) of 1-D Plug Flow Reactors (PFR), whose characteristic length is determined by the residence time in the particular reformer section. In order to obtain accurate residence time distribution across the reformer the following procedure was adopted. The non-reacting high temperature turbulent flow field inside the reformer is simulated in a two stage process. The first stage involves a 2D simulation of the "entire" flow field incorporating an algebraic model for the calculation of pressure drop in a simplified wall flow filter domain. The second stage involves a full 3D simulation of the non-reacting flow inside the wall flow filter channel, in order to obtain a better estimate for the local residence time. In the final part of the paper a comprehensive detailed kinetic scheme for the high temperature methane oxidation is incorporated in the RN model so as to obtain species profiles distributions at the reformer exit as a function of the operating parameters.

Description of experimental setup and procedure

A schematic drawing of the experimental setup is presented in Figure 3. The setup includes the reformer, measurement instrumentation and the hardware for controlling operating parameters and acquiring experimental data. Pure methane 2.5 (>99.5%) and dry compressed air were supplied with calibrated mass flow controllers. Electrical preheating was employed via two preheaters. For proper mixing of the educts upstream of the reformer, a mixer was used that has been designed so as to eliminate problems of spontaneous mixture ignition and flame flashback [7]. The thermocouples T_{mix},T_4,T_5 and T_{ex2} were N-type with an Inconel protection sheath, T_{mix} was used for monitoring and controlling the temperature of the methane-air mixture. The temperature distribution within the reaction zone(empty conical section) was measured with the S-type thermocouples T_1, T_2 and T_3 protected by a ceramic sheath. Two N-type thermocouples, T_4 and T_5, were placed inside the wall flow filter at a distance of 30mm and 70mm from the filter exit, respectively. Also a K-type thermocouple, T_{ex1}, was placed immediately after the exit of the wall flow filter. Sensitive differential pressure transducers with a measurement range of 0-2500 Pa were utilized to continuously monitor pressure drop between inlet and outlet of the reformer and between inlet and outlet of the wall flow filter. Stainless steel probes were utilized for the collection of gas samples at the exit of the reformer. The probed sample was used to on-line analyze for the species H_2, CO, CO_2, CH_4, C_2H_2.

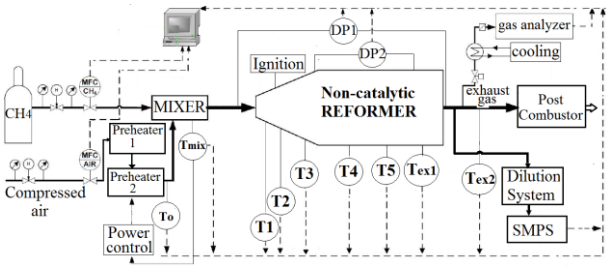

Figure 3: Flow sheet of the experimental setup.

The detection of soot particles and their particle size distribution (PSD) measurement was realized with a commercial Scanning Mobility Particle Sizer (SMPS) device (TSI Mobel 3080). For reliable PSD measurements a dilution system had to be designed for suitable sampling. The chemical reactions and gas phase kinetics in the sample have to be quenched fast and very close to the sampling position so as to minimize the particle losses due to coagulation, thermophoresis, condensation, etc. Taking into consideration the process characteristics and the geometrical restrictions of the examined application, a three-stage dilution method was setup with the aim to achieve a total dilution of$>10^4$.

During start-up, the system was electrically preheated to 400^{o}C for all cases. After the initial warm-up phase the reformer was ignited at a relatively high air to fuel ratio (λ=0.7) inside the conical section. The flame propagated and stabilized within the conical section. During transition from one test point to another, the reformer would run until completely stationary operation could be assured before any measurement was taken for evaluation.

The operating behavior of the reformer was scanned varying the air-to-fuel ratio from λ=0.4-0.5 and by varying the fuel flow to achieve equivalent thermal powers in the range of 1- 4 kW. For all tested points the temperature profiles within the reformer and exhaust gas compositions were recorded. Furthermore, soot particle size distributions were measured for selected conditions. Gas samples were scanned by the SMPS in intervals of 90s. Following that, 10 samples were taken

with a scanning time of 100 s and were averaged to obtain the final distribution. Soot particle measurements were performed at a power of 1.5 kW (830 kW/m^2) and the air-to-fuel ratio variation started from λ=0.5 and decreased to λ=0.46 and λ=0.42. For λ=0.42 evidence of soot formation was detected. The air ratio was consecutively increased to λ=0.5 and λ=0.6 where self-regeneration was detected. For species measurements, the sampled gas was allowed to cool down, dried and transported to the gas analyzer. Water concentration was calculated from species balance and the mass balance of oxygen.

Experimental results

Temperature profiles and major species

Temperature profiles are presented in Figure 4. The temperature levels increase as a function of λ and the maximum temperature is an indication of flame stabilization. The profiles show how the variation in cross-section area affects the process of flame stabilization within the reformer. The variation of operating conditions leads to a new flame position. In the case of 2 kW and λ=0.4 the stabilization position has completely shifted out of the conical section and the reaction front lies inside the wall flow filter. Such a case results in much shorter gas residence times within the post flame zone, which results in poorer regeneration.

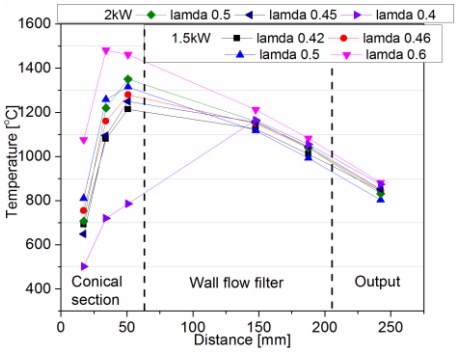

Figure 4: Temperature profiles for different λ and thermal loads of 1.5 kW and 2kW.

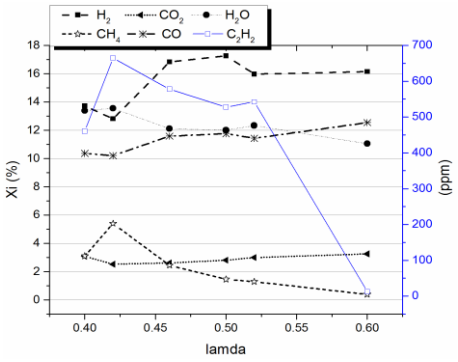

Figure 5: Wet syngas composition for different λ.

The gas composition is presented in Figure 5 for the case of 1.5 kW and for different air ratios. The measured major species H_2, CO, CO_2 and minor species CH_4, C_2H_2 concentrations were rescaled on the basis of the calculated mole flow of wet syngas for each case of air ratio. Carbon and hydrogen balances were calculated and they were found to close for all examined cases.

Regeneration and reforming efficiency

Pressure drop is an indirect index of soot accumulation within the filter. The evolution of pressure drop along the wall flow filter as function of time, for thermal load 1.5 kW and different air ratios is illustrated in Figure 6. The pressure drop was found to increase for λ = 0.42 and this is evidence of soot. The temperature inside the wall flow filter was about 1200°C. The regeneration point was observed after increasing λ to 0.5, where the temperature was about 1300°C.

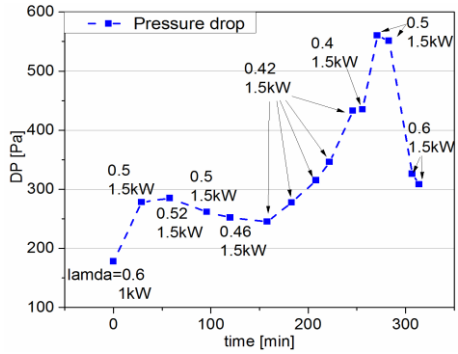

Figure 6: Filter pressure drop as function of time and λ.

Figure 7 illustrates species mole fractions for all tested cases as a function of time and air ratio. Mole fractions of H_2, CO and CH_4 increase by decreasing the air ratio. However, for λ=0.42, where the soot point appeared, the mole fractions of H_2, CO decreased and those of H_2O, CH_4 increased respectively. Thereafter, by setting the air ratios to 0.5 and 0.6, soot regeneration took place and an increase in H_2, CO as well as a decrease in H_2O mole fractions was observed. These trends indicate the activity of Boudouard reactions during regeneration.

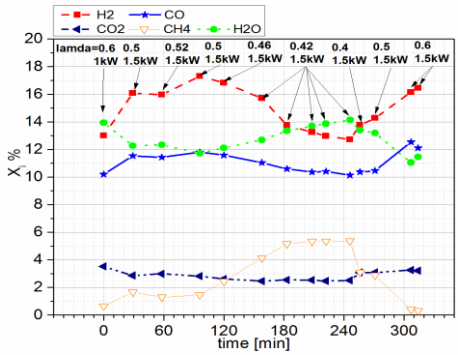

Figure 7: Wet syngas composition as a function of time and λ for 1 kW and 1.5 kW.

The comparison of pressure drop and acetylene profiles corroborates a causal connection between acetylene concentration and soot formation. As illustrated in Figure 8 a significant amount of acetylene was measured for λ = 0.5. However, when the soot point appeared for λ=0.42 (Figure 6) the acetylene mole

fraction had a steep decrease, possibly due to consuming reactions leading to intermediate soot precursor species, followed by a time interval of non-changing concentrations, indicating a dynamic equilibrium between acetylene and soot. Increasing air ratios under regeneration conditions acetylene levels were decreased and eventually eliminated.

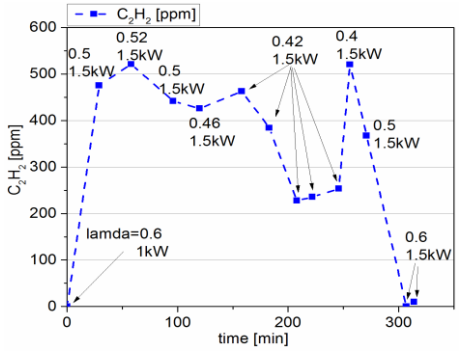

Figure 8: Acetylene concentration as function of time and λ, for 1 and 1.5kW.

A total reforming efficiency can be calculated on the basis of the formula:

$$n_{ref} = \frac{\dot{n}_{H_2} LHV_{H_2} + \dot{n}_{CO} LHV_{CO}}{\dot{n}_{CH4} LHV_{fuel}} \times 100\% \quad eq.(1)$$

For the given conditions, at an air ratio of λ=0.5, an efficiency of 65% was calculated. Figure 9 illustrates the efficiency for all tested conditions as function of air ratio and time. It is noted that the efficiency decreases significantly to 44% after 2 hours, when the soot point appears for λ=0.42 and sharply increases during soot regeneration to 76%.

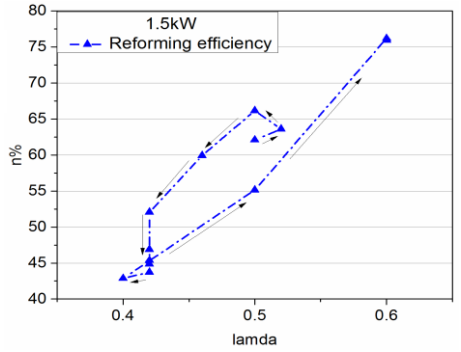

Figure 9: Reforming efficiency as function of time and λ.

Soot measurements

The electrical mobility diameter distributions of the detected soot particles within the exhaust gas of the reformer is illustrated in Figure 10. Distributions have been corrected for diffusion losses within the electrostatic classifier and scaled back to flame conditions by accounting for dilution and cooling of the examined samples. Some of the important characteristics of the presented distributions, such as mean diameter, standard deviation, particle number density and mass density have been summarized in Table 1 and they have been sorted according to the time sequence of the experimental procedure. The results show that the majority of the detected particles are sized in the range of 10 nm up to 110 nm. The mean diameter increases by decreasing air ratio. The particle number concentration are expected to increase for lower air ratios. However, in the cases from λ=0.46-0.42, the number concentration decreases, due to the fact that bigger particles appear and the efficiency of wall flow filter in retaining particles increases. Increasing the air ratio to λ=0.5 starts the regeneration. The agglomerates start to decompose and a larger number of particles is measured. Increasing the air ratio to λ=0.6 results in no particle detection.

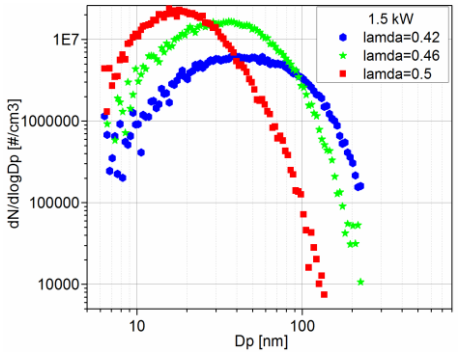

Figure 10: Soot particle size distributions as function of λ.

Table 1:Particle mean diameter, number and mass concentration for different air-to-fuel ratios.

λ	Mean particle diameter Dp [nm]	Standard deviation σ	Number concentration [#/cm^3]	Mass concentration [mg/cm^3]
0.5	21.25	1.60	1.17E+07	1.53E-04
0.46	38.35	1.79	1.11E+07	1.63E-04
0.42	51.87	1.97	4.85E+06	3.71E-04
0.5	17.47	1.65	3.33E+09	5.40E-07
0.6	No particles detected	No particles detected	No particles detected	No particles detected

Numerical modeling

Pressure drop model

The 2D axisymmetric model of the entire reformer was used to obtain mean residence time τ_{res} calculations in the four reformer sections depicted in Fig. 2. Computations were conducted using ANSYS FLUENT 14.0 [9]. The filter domain was simulated as a porous packed bed. The required coefficients K_{an} and C_2 in (eq. 2) for pressure drop in packed bed simulation used by FLUENT were derived as a function of the geometrical and flow characteristics of the filter, eq.(4, 5).These expressions were derived by combining an algebraic equation for wall flow filter pressure drop, eq. (3), [8] and the pressure drop equation (eq.2).

$$\Delta P_{an} = \left(\frac{\mu_{in}}{K_{an}} U_{in} + C_2 \frac{1}{2} \rho_{in} {U_{in}}^2\right) L \qquad \mathbf{eq.(2)}$$

$$\Delta P_{al} = \frac{\mu_{ex} \dot{Q}_{oex}}{20 V_o} (a+w)^2 \left(\frac{w}{k_o a}\right) + \frac{\mu_{ex} \dot{Q}_{oex}}{20 V_o} (a+w)^2 \left(\frac{8\, F\, L^2}{3\, a^4}\right) \mathbf{eq.(3)}$$

$$K_{an} = \frac{\mu_{in} \rho_{ex} \dot{Q}_{ex}\ 20\, L V_0 K_o a}{\mu_{ex} \rho_{in} A \dot{Q}_{oex} (a+w)^2 w} \mathbf{eq.(4)}$$

$$C_2 = \frac{\mu_{ex} \dot{Q}_{oex}\ 16\, L F \rho_{in} A^2 (a+w)^2}{60\, V_o a^4 \rho_{ex}{}^2 \dot{Q}_{ex}} \mathbf{eq.(5)}$$

The 2D computations indicate a uniform flow field inside the filter section, which is not realistic. In order to capture flow effects introduced by the filter geometry and potentially obtain a better estimate for the corresponding residence time, 3D simulations were performed in a wall filter channel as shown in Fig. 12.

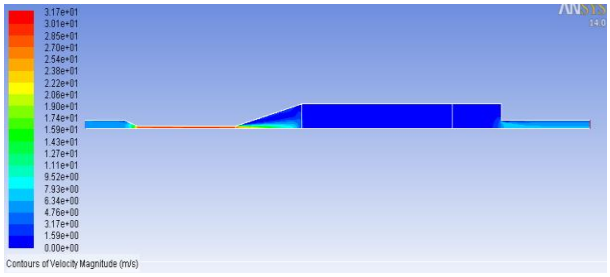

Figure 11: The 2D axisymmetric velocity field of the reformer.

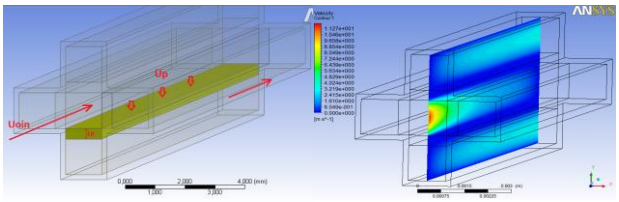

Figure 12: 3D model of a filter channel and the calculated velocity field.

This provides a realistic representation of the geometry and the flow in each channel. The one end of the rectangular channel is open to the flow while the other end is closed by a non-permeable material, modeled here as a solid wall. The four side walls of the channel are porous and permeable. The computational domain consists of four such channels, as also shown in Fig. 12. The external walls of the assembly are also assumed to be solid. The flow enters the channel with a velocity component parallel to the filter main axis, hits the solid wall at the other end of the channel and is forced to acquire a perpendicular component through the four porous side walls and eventually move into the four side channels. As a result soot particles can be retained in the porous walls and naturally the overall flow residence time is increased. The four porous walls are simulated as porous packed beds with the same K_{an} and C_2. Compared to the 2D case average values of $\bar{\rho}_{in}, \bar{\mu}_{in}, \overline{U}_p$ have to be used and the pressure drop FLUENT equation assumes the form shown in (eq. 6). The K_{an} and C_2 equations (7, 8) are derived by combining (eq.6) and (eq.3). A linear variation of density and viscosity as a function of temperature is assumed along the length of the channel, based on the experimental inlet and outlet temperature values, while an iterative procedure is followed for estimating the velocity distribution aiming to derive K_{an} and C_2 values that reproduce the experimental pressure drop along the wall flow filter.

$$\Delta P_{an} = L_p \frac{\bar{\mu}_{in}}{K_{an}} \bar{U}_p + C_2 \frac{1}{2} \bar{\rho}_{in} \bar{U}_p{}^2 L_p \quad \textbf{eq. (6)}$$

$$K_{an} = \frac{L_p \bar{\mu}_{in} \bar{U}_p 20\, V_o K_o a}{\mu_{ex} \dot{Q}_{oex} (a+w)^2 w} \quad \textbf{eq. (7)}$$

$$C_2 = \frac{\mu_{ex} \dot{Q}_{oex} (a+w)^2 16\, FL^2}{\bar{\rho}_{in} \bar{U}_p{}^2 L_p 20 V_o 3\, a^4} \quad \textbf{eq. (8)}$$

Pulse method for mean residence time calculation

The mean residence time τ_{res} was calculated for the 3D and 2D models by the following procedure. First, the flow field is calculated via a steady state simulation and the mass, momentum and energy equations are solved. Subsequently, the steady state solution is used as an initialization for a transient simulation where a scalar transport equation for a tracer (air) is solved. The tracer is injected in the first time step (tracer mass fraction at inlet = 1). For the remaining time steps the tracer mass fraction at the inlet is set to zero and the tracer transport equations are solved. The area-weighted average "tracer" mass fraction, C(t), (eq.9) is recorded at selected cross sections (see Fig.2) for the 2D model and at the exit of the filter channel for the 3D model. The mean residence time is calculated by (eq. 10).

$$C = \frac{1}{A} \int \Phi dA = \frac{1}{A} \sum_{i=1}^{n} \Phi_i |A_i| \quad \textbf{eq. (9)},$$

$$\bar{t} = \frac{\sum t_i C_i}{\sum C_i} \quad \textbf{eq. (10)}$$

The spatial and time solution independence for 2D and 3D simulations was for time steps of 10^{-5} and 10^{-4}s and for $9 \cdot 10^4$ and $7 \cdot 10^6$ nodes respectively. Simulations are presented for isothermal air flow for the case of a thermal load of 1.5kW and λ=0.6. Steady state velocity flow fields for 2D and 3D simulations are depicted in Figures 11 and 12 respectively. The introduction of a detailed description of the filter channels provides a more realistic representation of the flow field, e.g. at least qualitatively captures the flow penetration in adjacent channels, and modifies the mean residence time in the filter from a value of τ_{res}=89.3ms, in the 2D simulation, to a value of τ_{res}=138.1ms, in the 3D simulation. This 50% increase is clearly a better estimate as it reflects the complexity of the flow.

Reactor Network

Reactor network simulations were carried out using the CHEMKIN 4.1 [10] software. The obtained reactor network is depicted in Figure 13 and consists of a series of plug flow reactors (PFR). Plug flow calculations assume no velocity, temperature, or species gradients in the radial reactor direction. The length of each PFR was calculated based on the mean residence times obtained by the above methodology. CFD simulations. The characteristic PFR lengths and the corresponding residence times are presented in Table 2.

Table 2: Calculated mean residence times and characteristic PFR lengths in the reformer RN.

	Mean residence time [sec]	Characteristic PFR lengths [mm]
Conical /C2	0.0421	73
Filter /C3	0.1381	95
Exit1 /C4	0.07224	37
Exit2 /C5	0.01386	90

The RN was solved with the detailed kinetic mechanism of Vourliotakis et.al [11]. The mechanism

consists of 142 species and 820 elementary reactions. The experimental temperature profile was used for the calculations. Figure 14 illustrates the numerical results of species distributions along reformer in comparison with the experimental measurements of wet syngas composition at the reformer exit, for the case of 1.5kW and λ=0.6.

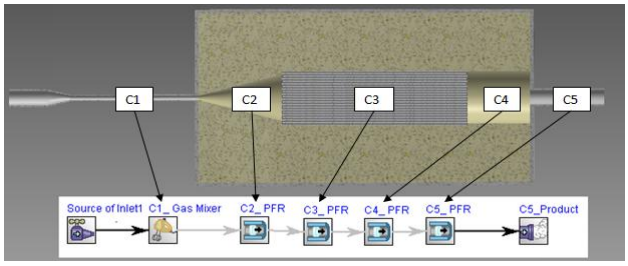

Figure 13: The reformer reactor network.

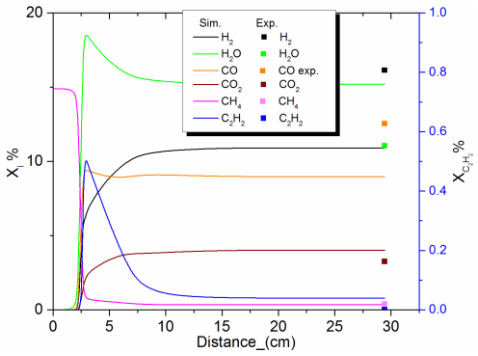

Figure 14: Calculated species distribution along the reformer and experimental measurements at the reformer exit.

Conclusions

An experimental and numerical investigation of a novel non-catalytic reformer design was carried out. The reformer shows the potential of both soot passive regeneration combined and high reforming efficiency that can reach up to 65%. Appropriate numerical models for pressure drop and mean residence time calculation in the wall flow filter have been developed and incorporated in 2D and 3D CFD models. An equivalent Reactor Network (RN) was formulated on the basis of CFD simulations in order to incorporate detailed gas-phase chemistry in the calculations. Predicted major species levels at the reformer exhaust were found to be acceptable.

Acknowledgments

SB and MF acknowledge the JTI–FCH-JU-1 HELMETH project for its financial support. GS acknowledges financial support through the ERA-NET CAPITA CARDIOSOL project.

References

[1] Bharadwaj S.S., L. D. Schmidt, *Fuel Process Technol.* 42 (1995) 109-127.
[2] G. Vourliotakis, G. Skevis, M.A. Founti, Z. Al-Hamamre, D. Trimis, *Int. J. Hydrogen Energ.* 33(2008) 2816-2825.
[3] A. Loukou, I. Frenzel, J. Klein, D.Trimis, *Int. J. Hydrogen Energ.*37 (2012) 16686-16696.
[4] J.M.C. Pereira, M.A.A. Mendes, D. Trimis, J.C.F. Pereira, *Fuel*89 (2010) 1928-1935.
[5] A.Raimondi, A.Loukou, D.Fino, D.Trimis, Chem. Eng. J.176-177 (2011) 295-301.
[6] A. Raimondi, D. Fino, G. Saracco, *J. PowerSources* 193 (2009) 338-341.
[7] Z. Al-Hamamre, S. Voß, D. Trimis, *Int. J. Hydrogen Energ.*34 (2009) 827-832.
[8] E. Kladopoulou, S. Yang, J. Johnson, G. Parker, A.G. Konstandopoulos,*SAE Technical Paper* (2003)-01-0842.
[9] ANSYS/FLUENTv14.0,ANSYS Inc.
[10] CHEMKINCollection, Release 4.1. San Diego, CA: Reaction Design Inc.
[11] G. Vourliotakis ,G.Skevis, M.A Founti., *P. Combust. Inst.* 35(2015) 437-445.

Nomenclature

ΔP_{an}	Pressure drop of porous packed bed	[Pa]
ΔP_{al}	Pressure drop of wall flow filter given by algebraic model	[Pa]
L_p	Length of porous packed bed or width of wall's flow filter	[m]
$\bar{\mu}_{in}$	Average viscosity in filter channel wall	[kg/m*sec]
K_{an}	Viscous resistance	[1/m^2]
$\bar{U}_p$	Average velocity in filter channel wall	[m/s]
C_2	Inertial resistance	[1/m]
$\bar{\rho}_{in}$	Average density in filter channel wall	[kg/m^3]
μ_{ex}	Viscosity at the exit of wall flow filter	[kg/m*sec]
$\dot{Q}_{oex}$	Volume flow at the exit of filter's channel	[m^3/s]
V_o	Volume of channel	[m^3]
a	Filter cell width	[m]
w	Wall thickness	[m]
k_o	Permeability of wall flow filter	[m^2]
F	Constant of algebraic model for pressure drop of wall flow filter	[-]
L	Length of wall flow filter	[m]
μ_{in}	Viscosity in the inlet of wall flow filter	[kg/m*sec]
U_{in}	Velocity in the inlet of wall flow filter	[m/sec]
ρ_{in}	Density in the inlet of wall flow filter	[kg/m^3]
$\dot{Q}_{ex}$	Volume flow at exit of wall flow filter	[m^3/sec]
A	Cross section of porous packed bed	[m^2]
LHV	Lower Heating Value	[kj/kmole]
$\dot{n}$	Volume flow	[kmole/sec]
λ	Air-to-fuel ratio (lamda)	
C	Area-weighted average of tracer mass fraction	[kg/kg]
Φ	Scalar quantity (air)	[kg/kg]
$\bar{t}$	Mean residence time	[sec]
X	Mole fraction	[mole/mole]
D_p	Particle diameter	[nm]
$dN/dlogD_p$	Normalized number concentration	[#/cm^3]

Subscripts

an	Refers to an ANSYS equation
al	Refers to an algebraic model
p	Porous or Particle
in	Inlet
ex	Exit of the wall flow filter
oex	Exit of a channel of the wall flow filter
o	Refers to one channel of wall flow filter
i	Refers in a chemical species or in a discrete quantity